IEEE Access
Multidisciplinary | Rapid Review | Open Access Journal

Received April 5, 2022, accepted April 15, 2022, date of publication April 18, 2022, date of current version April 25, 2022.

Digital Object Identifier 10.1109/ACCESS.2022.3168564

Filtering-Error Constrained Angle Tracking Adaptive Learning Fuzzy Control for Pneumatic Artificial Muscle Systems Under Nonzero Initial Errors

XIAOHUI GUAN[1], ZHONGJIE HE[2], (Member, IEEE), MEIYAN ZHANG[3], AND HUIJIE XIA[1]

[1]College of Information Engineering, Zhejiang University of Water Resources and Electric Power, Hangzhou 310018, China
[2]School of Automation, Hangzhou Dianzi University, Hangzhou 310018, China
[3]College of Electrical Engineering, Zhejiang University of Water Resources and Electric Power, Hangzhou 310018, China

Corresponding author: Xiaohui Guan (guanxh1977@163.com)

This work was supported in part by the National Natural Science Foundation of China under Grant 61801431, in part by the Zhejiang Provincial Basic Public Welfare Research Plan of China under Grant LGF20F020007, and in part by the Zhejiang Provincial Natural Science Foundation of China under Grant LGG20F030003 and Grant LZJWY22E090001.

ABSTRACT In this paper, a filtering-error constrained adaptive iterative learning control scheme is proposed to solve the angle tracking problem for a pneumatic artificial muscle-actuated mechanism. The adaptive learning controller is designed by a novel barrier Lyapunov function, and the filtering error of pneumatic artificial muscle system is ensured to be constrained during each iteration. The initial position problem of iterative learning control is solved by utilizing time-varying boundary layer method. Fuzzy logic system is applied to approximate the unknown nonparametric uncertainties in the pneumatic artificial muscle system, whose optimal weight is estimated by using difference learning approach. The approximation error of fuzzy logic system is tackled by robust control strategy. Simulation results show the effectiveness of the propose angle tracking adaptive learning fuzzy control scheme.

INDEX TERMS Pneumatic artificial muscle systems, adaptive iterative learning control, barrier Lyapunov function, initial position problem, fuzzy logic systems.

I. INTRODUCTION

Currently, by virtue of the excellent flexibility and compliance, soft robots have been widely used in rehabilitation robotics, prosthetic robots and the human-robot interaction. With the development of soft robots, soft actuators earn increasing interests as the formers' important components. Pneumatic artificial muscle (PAM) is a tube-like actuator and can largely mimic the functions of human muscles by inflating and deflating pressurized air through servo valves [1], [2]. PAM actuator may be seen as one of the most promising soft actuators for many advantages including rapid response, low cost and high power weight ratio. These merits have fueled the wide industrial applications for PAM actuators [3]–[6], [8]–[10], [44]. For the sake of existing inherent hysteresis, high nonlinearities and creep characteristics, the accurate modeling and control for PAM system is not an easy job, and the applicability of some existing control algorithms is limited. Therefore, in order to get better control performance, it is of urgent need to introduce new control design methods for decreasing the PAM-actuated mechanisms' sensitivity to dynamic uncertainties in practice.

Iterative learning control (ILC) is effective in handling repeated control processes [11]–[17], [17], [19], [20]. The ILC system can obtain excellent performances through gradual iterative learning, with little system model knowledge used [21]–[24]. Usually, PAM-actuated rehabilitation mechanisms are used to perform repeated tasks over a fixed period of operation time. Thus, ILC is a potential suitable control technique for obtaining accurate tracking. We will consider two important aspects of ILC algorithm designs for PAM systems in this work.

The first aspect is about the initial position problem of PAM systems. Many traditional ILC theoretical algorithms

The associate editor coordinating the review of this manuscript and approving it for publication was Bidyadhar Subudhi.

can perform well under zero initial error condition, but they perform poorly if this condition cannot be satisfied. More specifically, error divergence probably happens even if the initial error is very slight. Note that resetting the initial value of system state/output exactly to that of reference trajectory at each iteration is an impossible task in real applications. Hence, the zero initial error condition is too strict to be met in applications. The issue on how to develop iterative learning controller under nonzero initial condition, which is the so-called initial position problem of ILC, is a fundamental problem in ILC area. In order to solve this problem of ILC, some significant explorations and attempts have been made in the past two decades [25]–[30]. Up to now, the documents discussing the ILC approach for PAM systems are very few, and the documents have reported the result involving initial position problem of ILC for PAM systems are even fewer. In [31], a model-free discrete adaptive ILC method is proposed for nonlinear PAM systems. In [32], alignment condition is used to relax the initial position problem for PAM systems whose reference trajectory is smoothly closed, i.e., the proposed approach is suitable for the case that the initial state of reference trajectory is equal to the final state of reference trajectory. How to develop an effective control scheme for PAM systems whose reference trajectory is not closed is still unclear.

The second issue we will address in this work is about system constraints of PAM systems during operations. Due to the system specifications and safety considerations, there exist the requirements of constraining the system output, the system state, or the output tracking error in some situations. Some related results have been reported in literature, such as maximal output admissible set strategy [33], constrained model predictive control [34], reference governor approach [35], convex optimization strategy [36] and barrier Lyaponov function design method [37], [38]. In recent years, the system constrain problem in ILC design has attracted much interest. By referring to the state/output constraint technique in barrier adaptive control, the research results on barrier adaptive ILC have been reported in literature since the early 2010s. In [39], Jin *et al.* proposed an output-constrained adaptive ILC approach for a class of nonlinear systems which meets alignment condition. In [40], Yan and Sun presented an error-tracking iterative learning control method for a class of nonparametric uncertain systems to tackle simultaneously both the initial position problem and the state-constrained problem. In [41], Yu *et al.* developed an adaptive ILC algorithm for nonlinear uncertain systems with both state and input constraints. In [42], Jin investigated the joint position constrained ILC for robotic systems. Up to now, few literature has addressed the system constraint problem in the adaptive ILC for PAM systems.

Motivated by the above discussion, this work focuses on the adaptive ILC algorithm design for the angle tracking of PAM systems under nonzero initial errors with filtering error constraint. The main results and contributions are given as follows.

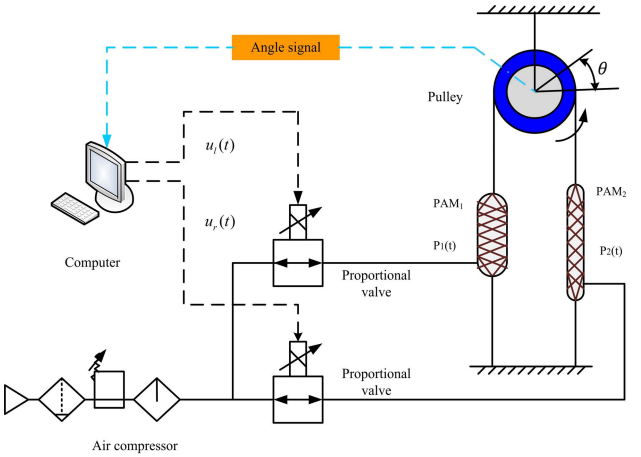

FIGURE 1. Control system structure of the PAM-actuated mechanism.

1) The filtering-error constraint in adaptive ILC for PAM systems is implemented by using a new type of barrier Lypunov function in ILC design.
2) Time-varying boundary layer and adaptive learning fuzzy logic system are jointly applied to deal with the initial position problem and uncertainties in PAM ILC systems. An adaptive ILC law is developed to make the angle tracking error converge to a tunable residual set as the iteration number increases.
3) In many existing related results, the state dependent control input gain in system model is assumed to be state independent, which is relaxed in this work.

The paper is organized as follows. Section II introduces the control problem formulation and some preliminaries. In Section III, we propose the filtering-error constrained angle tracking adaptive learning fuzzy control scheme for PAM systems under nonzero initial errors via using the techniques of barrier Lyapunov function, time-varying boundary layer, and fuzzy logic system. The convergence analysis of closed-loop PAM systems is given in Section IV. In Section V, some simulation results are illustrated to verify the effectiveness of the proposed control scheme. Finally, Section VI concludes this work.

II. PROBLEM FORMULATION

A. SYSTEM DESCRIPTION

In this work, the angle trajectory tracking problem is considered for a PAM-acutated mechanism [2], which is used to perform repeated tasks. The control system structure of the mechanism is shown in Fig. 1.

As shown in this figure, the main components include an computer, an air compressor, two proportional valves, two PAM actuators and an angle sensor. Two PAM actuators are parallel to each other. Through opening and closing of two pressure proportional valves, the charging or discharging of two PAM actuators are controlled by the computer. The signals of deflection angles are transmitted to the computer through an angle sensor. The two control variables of the

PAM-actuated mechanism are presented as

$$\begin{cases} u_l(t) = u_o + \alpha_u u(t), \\ u_r(t) = u_o - \alpha_u u(t), \end{cases} \tag{1}$$

where $t \in [0, T]$, α_u is the coefficient of voltage distribution, u_o is the preloaded voltage, $u(t)$ is the control input, and $u_l(t)$ and $u_r(t)$ are two input control voltages of pressure proportional valves, respectively. Here, T represents the interval of operation time at each iteration. The internal pressures of two PAM actuators are given as

$$\begin{cases} P_1(t) = P_0 + \Delta P(t) = \alpha_0 u_l(t), \\ P_2(t) = P_0 - \Delta P(t) = \alpha_0 u_r(t), \end{cases} \tag{2}$$

where α_0 is the proportional coefficient of the control voltage and output pressure. P_0 denotes the preload internal pressure of actuators, $\Delta P(t)$ represents the variation of pressure, and $P_1(t)$ and $P_2(t)$ are two internal pressures of PAM actuators. The relationship between the pulling forces and the internal pressures of PAM actuators may be described as

$$\begin{cases} F_1(t) = P_1(t)(\alpha_1\epsilon_1^2(t) + \alpha_2\epsilon_1(t) + \alpha_3) + \alpha_4, \\ F_2(t) = P_2(t)(\alpha_1\epsilon_2^2(t) + \alpha_2\epsilon_1(t) + \alpha_3) + \alpha_4, \end{cases} \tag{3}$$

where $F_1(t)$ and $F_2(t)$ are two pulling forces of PAM actuators, $\alpha_1, \alpha_2, \alpha_3$ and α_4 are four parameters, $\epsilon_1(t) = \epsilon_0 + rl_0^{-1}\theta(t)$ and $\epsilon_2(t) = \epsilon_0 - rl_0^{-1}\theta(t)$. Here, $\theta(t)$ denotes the deflection angle of the mechanism, ϵ_0 and l_0 represent the initial shrinking rate and the initial length of PAM actuators, respectively. The driving moment of this mechanism is shown as

$$T_p(t) = J\ddot{\theta}(t) + b_\upsilon\dot{\theta}(t) = F_1(t)r - F_2(t)r + d_\upsilon(\theta, \dot{\theta}, t), \tag{4}$$

where J is the moment of inertia, b_υ is the damping coefficient, r is the radius of pulley, and $d_\upsilon(\theta, \dot{\theta}, t)$ denotes the unknown external disturbances and unmodeled dynamics. By substituting (1)-(3) into (4), we have

$$\begin{aligned} \ddot{\theta}(t) = & -J^{-1}b_v\dot{\theta}(t) + 2Jk_0u_or^2(2\alpha_1\epsilon_0 + \alpha_2)l_0^{-1}\theta(t) \\ & +2J^{-1}k_0\alpha_u r[\alpha_1\epsilon_0^2 + \alpha_2\epsilon_0 + \alpha_3 + 2\alpha_2\epsilon_0 \\ & +\alpha_1(r\theta(t)l_0^{-1})^2]u(t) + d_s(\theta, \dot{\theta}, t) \end{aligned} \tag{5}$$

where $d_s(\theta, \dot{\theta}, t) = J^{-1}d_\upsilon(\theta, \dot{\theta}, t)$. Let $x_1(t) = \theta(t)$ and $x_2(t) = \dot{\theta}(t)$. Then, the state-space model of the PAM system at the kth iteration may be got as follows:

$$\begin{cases} \dot{x}_{1,k}(t) = x_{2,k}(t), \\ \dot{x}_{2,k}(t) = u_{o,k}h_1x_{1,k}(t) + h_2x_{2,k}(t) + [g_1 \\ \qquad\qquad +g_2x_{1,k}^2(t)]u_k(t) + d_s(\boldsymbol{x}_k, t), \end{cases} \tag{6}$$

where $h_1 = 2J^{-1}k_0r^2(2\alpha_1\epsilon_0 + \alpha_2)l_0^{-1}$, $h_2 = -J^{-1}b_v$, $g_1 = 2J^{-1}k_0\alpha_u r(\alpha_1\epsilon_0^2 + \alpha_2\epsilon_0 + \alpha_3)$, $g_2 = 2J^{-1}k_0\alpha_u r\alpha_1(rl_0^{-1})^2$, $\boldsymbol{x}_k = [x_{1,k}, x_{2,k}]^T$.

The control task of this work is to make $x_{1,k}(t)$ accurately track its reference signal $x_{1,d}(t)$ over $[0, T]$, as the iteration index k increases. For the sake of brevity, the arguments in this paper are sometimes omitted when no confusion is likely to arise.

Remark 1: In many results, the term $\alpha_1(r\theta(t)l_0^{-1})^2u(t)$ in (5) is assumed to be zero or bounded before controller design. In this work, we give up this usual assumption.

B. FUZZY LOGIC SYSTEMS

All is well known, fuzzy logic system (FLS) or neural network-based controller has become an important approach for adaptive control [8]–[44], [44]–[47] and adaptive learning control while the nonlinearity in nonlinear plants cannot be linearly parameterizable as in [25], [48], [49]. A typical FLS consists of four main components: knowledge base, fuzzifier, fuzzy inference engine and defuzzifier. The fuzzy inference mechanism uses the fuzzy IF-THEN rules to perform a mapping from an input vector $\boldsymbol{\chi} = [\chi_1, \chi_2, \cdots, \chi_n]^T \in U \subseteq \mathbb{R}^n$ to an output variable $y \in \mathbb{R}$, where $U = U_1 \times U_2 \times \cdots \times U_n$, with $U_i \in \mathbb{R}$ for $i = 1, 2, \cdots, n$. Let $\mathcal{F}_1^{j_i}$ be the fuzzy sets defined on the universe of discourse of the ith input for $j_i = 1, 2, \cdots, N_i$, then the fuzzy logic system is characterized by several if-then rules:

$\mathcal{R}^l$: If χ_1 is $\mathcal{F}_1^{j_1}$ and χ_2 is $\mathcal{F}_2^{j_2}$ and $\cdots$ and χ_n is $\mathcal{F}_n^{j_n}$, Then $y = \mathcal{G}^l$, $(l = 1, 2, 3, \cdots, N)$, where $\mathcal{G}^l$ is a fuzzy set defined on $\mathbb{R}$, $j_i \in \{1, 2, \cdots, N_i\}$, the value of j_i is dependent of l for $i = 1, 2, \cdots, n$, and $N = \prod_{i=1}^n N_i$ is the total number of rules.

Let $\mu_{\mathcal{F}_i^{j_i}}(\chi_i)$ denote the membership functions of $\mathcal{F}_i^{j_i}$. By implementing the strategy of singleton fuzzification, center-average defuzzifcation and product inference, the output of fuzzy logic system can be formulated as

$$y(\boldsymbol{\chi}) = \frac{\sum_{l=1}^{N} \bar{p}_l \prod_{i=1}^{n} \mu_{\mathcal{F}_i^{j_i}}(\chi_i)}{\sum_{l=1}^{N} [\prod_{i=1}^{n} \mu_{\mathcal{F}_i^{j_i}}(\chi_i)]} \tag{7}$$

where $\bar{p}_l$ is the point at which the fuzzy membership function of $\mathcal{G}^l$ achieves its maximum value. Let

$$z_l(\boldsymbol{\chi}) = \frac{\prod_{i=1}^{n} \mu_{\mathcal{F}_i^{j_i}}(\chi_i)}{\sum_{j=1}^{N} [\prod_{i=1}^{n} \mu_{\mathcal{F}_i^{j_i}}(\chi_i)]}, \quad l = 1, 2, \cdots, N, \tag{8}$$

$\boldsymbol{p} = [\bar{p}_1, \bar{p}_2, \cdots, \bar{p}_N]^T$ and $\boldsymbol{z}(\boldsymbol{\chi}) = [z_1(\boldsymbol{\chi}), z_2(\boldsymbol{\chi}), \cdots, z_N(\boldsymbol{\chi})]^T$, then (7) can be rewritten as

$$y(\boldsymbol{\chi}) = \boldsymbol{p}^T\boldsymbol{z}(\boldsymbol{\chi}). \tag{9}$$

If Gaussian functions are adopted as the membership, then the following lemma holds.

Lemma 1: For amy real continuous function $f(\boldsymbol{\chi})$ defined on a compact set Ω in $\mathbb{R}^n$, there exists a FLS (9) and an optimal parameter vector $\boldsymbol{p}^*$ such that

$$\sup_{\boldsymbol{\chi} \in \Omega} |f(\boldsymbol{\chi}) - \boldsymbol{p}^{*T}\boldsymbol{z}(\boldsymbol{\chi})| \leq \varepsilon^*, \tag{10}$$

with ε^* being a arbitrary positive constant [43].

III. CONTROLLER DESIGN

By letting $e_1 = x_{1,k} - x_{1,d}$, $e_2 = x_{1,k} - x_{2,d}$ and $x_{2,d} = \dot{x}_{1,d}$, from (6), we have

$$\begin{cases} \dot{e}_{1,k} = e_{2,k}, \\ \dot{e}_{2,k} = u_{o,k}h_1x_{1,k}(t) + h_2x_{2,k}(t) + (g_1 \\ \qquad +g_2x_{1,k}^2(t))u_k + d_s(\boldsymbol{x}_k, t) - \ddot{x}_{1,d}. \end{cases} \tag{11}$$

Let $s_k = \lambda e_{1,k} + e_{2,k}$ and

$$s_{\phi,k}(t) = s_k(t) - \phi_k(t)\mathrm{sat}_{-1,1}\left(\frac{s_k(t)}{\phi_k(t)}\right), \tag{12}$$

where

$$\phi_k(t) = |s_k(0)|\mathrm{e}^{-\mu t}, \tag{13}$$

$\lambda > 0, \mu > 0$ and $\mathrm{sat}_{\cdot,\cdot}(\cdot)$ represents the definition of saturation function. For a scalar $\hat{a}$, which is the estimation to a scalar a,

$$\mathrm{sat}_{\underline{a},\bar{a}}(\hat{a}) := \begin{cases} \bar{a}, & \text{if } \hat{a} > \bar{a} \\ \hat{a}, & \text{if } \underline{a} \le \hat{a} \le \bar{a} \\ \underline{a}, & \text{if } \hat{a} < \underline{a}, \end{cases}$$

where $\underline{a}$ and $\bar{a}$ are the lower bound and upper bound of the scalar a, respectively. For a vector $\hat{\boldsymbol{a}} = [\hat{a}_1, \hat{a}_2, \cdots, \hat{a}_m] \in \mathbb{R}^m$, $\mathrm{sat}_{\underline{a},\bar{a}}(\hat{\boldsymbol{a}}) := \left[\mathrm{sat}_{\underline{a},\bar{a}}(\hat{a}_1), \mathrm{sat}_{\underline{a},\bar{a}}(\hat{a}_2), \cdots, \mathrm{sat}_{\underline{a},\bar{a}}(\hat{a}_m)\right]^T$.

Without loss of generality, we assume

$$d_s(\boldsymbol{x}_k, t) = d_1(\boldsymbol{x}_k) + d_2(\boldsymbol{x}_k, t),$$

where $d_1(\boldsymbol{x}_k)$ is continuous with respect to $\boldsymbol{x}_k$, and $d_2(\boldsymbol{x}_k, t)$ is the noncontinuous remainder with unknown bound. According to (11), the time derivative of s_k may be obtained as

$$\begin{aligned} \dot{s}_k = ce_{2,k} + u_{o,k}h_1x_{1,k} + h_2x_{2,k} + (g_1 + g_2x_{1,k}^2(t))u_k \\ +d_1(\boldsymbol{x}_k) + d_2(\boldsymbol{x}_k, t) - \ddot{x}_d. \end{aligned} \tag{14}$$

Let us choose a barrier Lyapunov function as

$$V_k(t) = \frac{s_{\phi,k}^2}{2(b_s^2 - s_{\phi,k}^2)^2}. \tag{15}$$

By defining $\varpi_{1,k} = b_s^2 + s_{\phi,k}^2$, $\varpi_{2,k} = b_s^2 - s_{\phi,k}^2$ and calculating the derivative of V_k with respect to t, according to (14), we have

$$\begin{aligned} \dot{V}_k(t) &= \frac{1}{2}\frac{2s_{\phi,k}\dot{s}_{\phi,k}}{\varpi_{2,k}^2} + \frac{1}{2}s_{\phi k}^2(-2)\varpi_{2,k}^{-3}(-2s_{\phi,k}\dot{s}_{\phi,k}) \\ &= \frac{s_{\phi,k}\dot{s}_{\phi,k}}{\varpi_{2,k}^2} + \frac{2s_{\phi,k}^2}{\varpi_{2,k}^3}s_{\phi,k}\dot{s}_{\phi,k} \\ &= \frac{\varpi_{1,k}}{\varpi_{2,k}^3}s_{\phi,k}[\dot{s}_k - \dot{\phi}_k(t)\mathrm{sgn}(s_{\phi,k})] \\ &= \frac{\varpi_{1,k}}{\varpi_{2,k}^3}s_{\phi,k}s_{\phi,k}\big[\alpha e_{2,k} + u_{o,k}h_1x_{1,k} + h_2x_{2,k} + gu_k \\ &\quad +d_1(\boldsymbol{x}_k) + d_2(\boldsymbol{x}_k, t) - \ddot{x}_d - \dot{\phi}_k(t)\mathrm{sgn}(s_{\phi,k})\big]. \end{aligned} \tag{16}$$

By using (12), we have

$$\begin{aligned} s_{\phi,k}\dot{\phi}_k(t)\mathrm{sgn}(s_{\phi,k}) &= s_{\phi,k}\mu\phi_k(t)\mathrm{sat}_{-1,1}\left(\frac{s_k(t)}{\phi_k(t)}\right) \\ &= \mu s_{\phi,k}(s_k - s_{\phi,k}). \end{aligned} \tag{17}$$

Substituting (17) into (16) yields

$$\begin{aligned} \dot{V}_k &= \frac{\varpi_{1,k}}{\varpi_{2,k}^3}s_{\phi,k}g_1\big[g_1^{-1}\lambda e_{2,k} + u_{o,k}g_1^{-1}h_1x_{1,k} + g_1^{-1}h_2x_{2,k} \\ &\quad +g_1^{-1}(g_1 + g_2x_{1,k}^2)u_k + g_1^{-1}d_1(\boldsymbol{x}_k) + g_1^{-1}d_2(\boldsymbol{x}_k, t) \\ &\quad -g_1^{-1}\ddot{x}_d + g_1^{-1}\mu(s_{\phi,k} - s_k)\big] \\ &= \frac{\varpi_{1,k}}{\varpi_{2,k}^3}s_{\phi,k}g_1[\boldsymbol{w}^T\boldsymbol{\xi}_k + g_1^{-1}(g_1 + g_2x_{1,k}^2)u_k] \\ &\quad +\frac{\varpi_{1,k}}{\varpi_{2,k}^3}s_{\phi,k}g_1(g_1^{-1}d_1(\boldsymbol{x}_k) + g_1^{-1}d_2(\boldsymbol{x}_k, t)), \end{aligned} \tag{18}$$

where $\boldsymbol{w} := [g_1^{-1}, g_1^{-1}h_1, g_1^{-1}h_2, g_1^{-1}\mu]^T$ and $\boldsymbol{\xi}_k := [\lambda e_{2,k} - \ddot{x}_d, u_{o,k}x_{1,k}, x_{2,k}, s_{\phi,k} - s_k]^T$.

Let $f(\boldsymbol{x}_k) = g_1^{-1}d_1(\boldsymbol{x}_k)$. According to Lemma 1, the unknown continuous function $g_1^{-1}d_1(\boldsymbol{x}_k)$ can be approximated by a suitable FLS with $\boldsymbol{x}_k \in \Omega_x$, where Ω_x is a compact set in $\mathbb{R}^2$. Then, we have

$$f(\boldsymbol{x}_k|\boldsymbol{\vartheta}_k) = \boldsymbol{\vartheta}_k^T(t)\boldsymbol{\varphi}(\boldsymbol{x}_k) + \epsilon(\boldsymbol{x}_k), \tag{19}$$

$$\boldsymbol{\vartheta}_k^*(t) = \arg\min_{\boldsymbol{\vartheta}_k}[\sup_{\boldsymbol{x}_k \in \Omega_x}(f(\boldsymbol{x}_k|\boldsymbol{\vartheta}_k) - f(\boldsymbol{x}_k))] \tag{20}$$

where $\boldsymbol{\vartheta}^*(t)$ is the the optimal fuzzy weight vector and $\boldsymbol{\vartheta}_k(t)$ is the estimate of $\boldsymbol{\vartheta}^*(t)$. The approximation error is defined as $\epsilon(\boldsymbol{x}_k) = f(\boldsymbol{x}_k|\boldsymbol{\vartheta}_k) - f(\boldsymbol{x}_k)$, where $|\epsilon(\boldsymbol{x}_k)| \le \epsilon_F$, with ϵ_F being a positive constant.

Denote $\boldsymbol{\varphi}(\boldsymbol{x}_k)$ briefly by $\boldsymbol{\varphi}_k$. Combining (18) with (19) leads to

$$\begin{aligned} \dot{V}_k = \frac{\varpi_{1,k}}{\varpi_{2,k}^3}s_{\phi,k}g_1[\boldsymbol{w}^T\boldsymbol{\xi}_k + g_1^{-1}(g_1 + g_2x_{1,k}^2)u_k] + \frac{\varpi_{1,k}}{\varpi_{2,k}^3} \\ \times s_{\phi,k}g_1(\boldsymbol{\vartheta}^{*T}(t)\boldsymbol{\varphi}_k + \epsilon(\boldsymbol{x}_k) + g_1^{-1}d_2(\boldsymbol{x}_k, t)). \end{aligned} \tag{21}$$

On the basis of (21), we design the control law and learning laws as follows:

$$u_k = u_{1,k} + u_{2,k}, \tag{22}$$

$$u_{1,k} = -\gamma_1\varpi_{2,k}s_{\phi,k} - \boldsymbol{w}_k^T\boldsymbol{\xi}_k - \boldsymbol{\vartheta}_k^T\boldsymbol{\varphi}_k, \tag{23}$$

$$u_{2,k} = -\frac{\varpi_{2,k}(\rho_k x_1^2|u_{1,k}| + \varrho_k)}{|\varpi_{2,k}|}\mathrm{sat}_{-1,1}\left(\frac{s_k(t)}{\phi_k(t)}\right) \tag{24}$$

$$\boldsymbol{w_k} = \mathrm{sat}_{\underline{w},\bar{w}}(\boldsymbol{w}_{k-1}) + \frac{\varpi_{1,k}}{\varpi_{2,k}^3}\gamma_2 s_{\phi,k}\boldsymbol{\xi}_k, \boldsymbol{w_{-1}} = 0, \tag{25}$$

$$\boldsymbol{\vartheta_k} = \mathrm{sat}_{\underline{\vartheta},\bar{\vartheta}}(\boldsymbol{\vartheta}_{k-1}) + \frac{\varpi_{1,k}}{\varpi_{2,k}^3}\gamma_3 s_{\phi,k}\boldsymbol{\varphi}_k, \boldsymbol{\vartheta_{-1}} = 0, \tag{26}$$

$$\rho_k = \mathrm{sat}_{0,\bar{\rho}}(\rho_{k-1}) + \frac{\varpi_{1,k}}{|\varpi_{2,k}|^3}\gamma_4|s_{\phi,k}|x_{1,k}^2|u_{1,k}|, \rho_{-1} = 0, \tag{27}$$

$$\varrho_k = \mathrm{sat}_{0,\bar{\varrho}}(\varrho_{k-1}) + \frac{\varpi_{1,k}}{|\varpi_{2,k}|^3}\gamma_5|s_{\phi,k}|, \varrho_{-1} = 0, \tag{28}$$

where $\gamma_1 > 0$, $\gamma_2 > 0$, $\gamma_3 > 0$, $\gamma_4 > 0$, $\gamma_5 > 0$, ρ_k is used to estimate $\rho := g_1^{-1}g_2$, and ϱ_k is used to estimate $\varrho(t) := \sup(\epsilon_F + g_1^{-1}|d_2(\boldsymbol{x}_k, t)|)$.

Remark 2: According to the definition of $s_{\phi,k}(t)$ given in (12) and (13), $s_{\phi,k}(0) = 0$ holds, which is useful for the formula derivation from (47) to (52). As shown in (15), barrier Lyaupunov function, rather than a traditional Lyapunov

function $V_k = \frac{1}{2}s_{\phi,k}(t)$, is used for controller design. The purpose is to let $s_{\phi,k}(t)$ constrained during each iteration as $s_{\phi,k}(t) < b_s$.

Remark 3: While the barrier Lyapunov function $V_{2,k} = \frac{1}{2}\frac{s_{\phi,k}^2}{b_s^2 - s_{\phi,k}^2}$ is adopted in controller design, one should check or prove the nonnegativity of $V_{2,k}$ in advance, which brings the inconvenience in controller design. This inconvenience may be removed by replacing $V_{2,k}$ with (15).

IV. CONVERGENCE ANALYSIS

Theorem 1: For the closed-loop PAM system composed of (6) and (22)-(28), the tracking performance and system stability are guaranteed as follows:

(1) The filtering error may be constrained in the sense that

$$|s_k(t)| < |s_k(0)|\mathrm{e}^{-\mu t} + b_s. \tag{29}$$

(2) $|e_{1,k}(t)| = \mathrm{e}^{-\lambda t}|e_{1,k}(0)| + \frac{\mathrm{e}^{-\mu t} - \mathrm{e}^{-\lambda t}}{\lambda - \mu}|s_k(0)|$ holds as the iteration number k increases.

(3) All adjustable control parameters $\boldsymbol{w}_k(t)$, $\boldsymbol{\vartheta}_k(t)$, $\rho_k(t)$, $\varrho_k(t)$, and internal signals $x_k(t), e_k(t), u_k(t)$ are bounded $\forall t \in [0, T]$ and $\forall k \geq 0$.

Proof: The proof consists of two parts. In Part A, we will prove that $|s_{\phi,k}| < b_s$ hold for any k. Then, we will analyze tracking error convergence in Part B.

Part A. The constraint property of s_k

Substituting (22) into (21) leads to

$$\begin{aligned}\dot{V}_k \leq & -\gamma_1 g_1 \frac{\varpi_{1,k}}{\varpi_{2,k}^2} s_{\phi,k}^2 + \frac{\varpi_{1,k}}{\varpi_{2,k}^3} s_{\phi,k} g_1 (\tilde{\boldsymbol{w}}_k^T \boldsymbol{\xi}_k \\ & + \tilde{\boldsymbol{\vartheta}}_k^T \boldsymbol{\varphi}_k) + \frac{\varpi_{1,k}}{|\varpi_{2,k}|^3}\left(|s_{\phi,k}| g_1 \rho x_{1,k}^2 |u_{1,k}| + |s_{\phi,k}| g_1 \varrho\right) \\ & - \frac{\varpi_{1,k}}{|\varpi_{2,k}|^3}|s_{\phi,k}|(g_1 + g_2 x_{1,k}^2) g_1^{-1} g_1 \rho_k x_{1,k}^2 |u_{1,k}| \\ & - \frac{\varpi_{1,k}}{|\varpi_{2,k}|^3}|s_{\phi,k}|(g_1 + g_2 x_{1,k}^2) g_1^{-1} g_1 \varrho_k, \end{aligned} \tag{30}$$

where $\tilde{\boldsymbol{w}}_k = \boldsymbol{w} - \boldsymbol{w}_k$ and $\tilde{\boldsymbol{\vartheta}}_k = \boldsymbol{\vartheta}^*(t) - \boldsymbol{\vartheta}_k$. Due to $s_{\phi,k}\mathrm{sat}_{-1,1}\left(\frac{s_k(t)}{\phi_k(t)}\right) = |s_{\phi,k}|$, $g_1 > 0$ and $g_2 > 0$, it follows from (30) that

$$\begin{aligned}\dot{V}_k \leq & -\gamma_1 g_1 \frac{\varpi_{1,k}}{\varpi_{2,k}^2} s_{\phi,k}^2 + \frac{\varpi_{1,k}}{\varpi_{2,k}^3} s_{\phi,k} g_1 (\tilde{\boldsymbol{w}}_k^T \boldsymbol{\xi}_k \\ & + \tilde{\boldsymbol{\vartheta}}_k^T \boldsymbol{\varphi}_k) + \frac{\varpi_{1,k}}{|\varpi_{2,k}|^3}\left(|s_{\phi,k}| g_2 x_{1,k}^2 |u_{1,k}| + |s_{\phi,k}| g_1 \varrho\right) \\ & - \frac{\varpi_{1,k}}{|\varpi_{2,k}|^3}\left(|s_{\phi,k}| g_1 \rho_k x_{1,k}^2 |u_{1,k}| + |s_{\phi,k}| g_1 \varrho_k\right) \\ = & -\gamma_1 g_1 \frac{\varpi_{1,k}}{\varpi_{2,k}^2} s_{\phi,k}^2 + \frac{\varpi_{1,k}}{\varpi_{2,k}^3} s_{\phi,k} g_1 (\tilde{\boldsymbol{w}}_k^T \boldsymbol{\xi}_k + \tilde{\boldsymbol{\vartheta}}_k^T \boldsymbol{\varphi}_k) \\ & + \frac{\varpi_{1,k}}{|\varpi_{2,k}|^3}\left(|s_{\phi,k}| g_1 \tilde{\rho}_k x_{1,k}^2 |u_{1,k}| + |s_{\phi,k}| g_1 \tilde{\varrho}_k\right) \end{aligned} \tag{31}$$

where $\tilde{\rho}_k = \rho - \rho_k$ and $\tilde{\varrho}_k = \varrho - \varrho_k$. According to (12), we can see $s_{\phi,k}(0) = 0$ holds. Define a barrier Lyapunov functional as follows:

$$L_k = V_k + \frac{g_1}{2\gamma_2}\int_0^t \tilde{\boldsymbol{w}}_k^T \tilde{\boldsymbol{w}}_k d\tau + \frac{g_1}{2\gamma_3}\int_0^t \tilde{\boldsymbol{\vartheta}}_k^T \tilde{\boldsymbol{\vartheta}}_k d\tau + \frac{g_1}{2\gamma_4}\int_0^t \tilde{\rho}_k^2 d\tau + \frac{g_1}{2\gamma_5}\int_0^t \tilde{\varrho}_k^2 d\tau. \tag{32}$$

With the help of (31), we can get the time derivative of L_k as

$$\begin{aligned}\dot{L}_k \leq & -\frac{\varpi_{1,k}^2}{\varpi_{2,k}^2}\gamma_{1,k} g_1 s_{\phi,k}^2 + \frac{\varpi_{1,k}}{\varpi_{2,k}^3} g_1 s_{\phi,k}(\tilde{\boldsymbol{w}}_k^T \boldsymbol{\xi}_k + \tilde{\boldsymbol{\vartheta}}_k^T \boldsymbol{\varphi}_k) \\ & + \frac{\varpi_{1,k}}{|\varpi_{2,k}|^3}\left(|s_{\phi,k}| g_1 \tilde{\rho}_k x_{1,k}^2 |u_{1,k}| + |s_{\phi,k}| g_1 \tilde{\varrho}_k\right) + \frac{g_1}{2\gamma_2} \\ & \times \tilde{\boldsymbol{w}}_k^T \tilde{\boldsymbol{w}}_k + \frac{g_1}{2\gamma_3}\tilde{\boldsymbol{\vartheta}}_k^T \tilde{\boldsymbol{\vartheta}}_k + \frac{g_1}{2\gamma_4}\tilde{\rho}_k^2 + \frac{g_1}{2\gamma_5}\tilde{\varrho}_k^2. \end{aligned} \tag{33}$$

By using (25), we have

$$\begin{aligned} & \frac{\varpi_{1,k}}{\varpi_{2,k}^3} s_{\phi,k} g_1 \tilde{\boldsymbol{w}}_k^T \boldsymbol{\xi}_k + \frac{1}{2\gamma_2} g_1 \tilde{\boldsymbol{w}}_k^T \tilde{\boldsymbol{w}}_k \\ & = \frac{g_1}{2\gamma_2}(\boldsymbol{w} - \boldsymbol{w}_k)^T (2\boldsymbol{w}_k - 2\mathrm{sat}_{\underline{w},\bar{w}}(\boldsymbol{w}_{k-1}) + \boldsymbol{w} - \boldsymbol{w}_k) \\ & = \frac{g_1}{2\gamma_2}[-\boldsymbol{w}_k^T \boldsymbol{w}_k + \boldsymbol{w}^T \boldsymbol{w} - 2\boldsymbol{w}^T \mathrm{sat}_{\underline{w},\bar{w}}(\boldsymbol{w}_{k-1}) \\ & \quad + 2\boldsymbol{w}_k^T \mathrm{sat}_{\underline{w},\bar{w}}(\boldsymbol{w}_{k-1})] \\ & = -\frac{g_1}{2\gamma_2}[\boldsymbol{w}_k - \mathrm{sat}_{\underline{w},\bar{w}}(\boldsymbol{w}_{k-1})]^T [\boldsymbol{w}_k - \mathrm{sat}_{\underline{w},\bar{w}}(\boldsymbol{w}_{k-1})] \\ & \quad + \frac{g_1}{2\gamma_2}[\mathrm{sat}_{\underline{w},\bar{w}}(\boldsymbol{w}_{k-1}^T)\mathrm{sat}_{\underline{w},\bar{w}}(\boldsymbol{w}_{k-1}) + \boldsymbol{w}^T \boldsymbol{w} \\ & \quad - 2\boldsymbol{w}^T \mathrm{sat}_{\underline{w},\bar{w}}(\boldsymbol{w}_{k-1})] \\ & \leq \frac{g_1}{2\gamma_2}[\mathrm{sat}_{\underline{w},\bar{w}}(\boldsymbol{w}_{k-1}^T)\mathrm{sat}_{\underline{w},\bar{w}}(\boldsymbol{w}_{k-1}) + \boldsymbol{w}^T \boldsymbol{w} \\ & \quad - 2\boldsymbol{w}^T \mathrm{sat}_{\underline{w},\bar{w}}(\boldsymbol{w}_{k-1})]. \end{aligned} \tag{34}$$

Note that each term in $\frac{g_1}{2\gamma_2}[\mathrm{sat}_{\underline{w},\bar{w}}(\boldsymbol{w}_{k-1}^T)\mathrm{sat}_{\underline{w},\bar{w}}(\boldsymbol{w}_{k-1}) + \boldsymbol{w}^T \boldsymbol{w} - 2\boldsymbol{w}^T \mathrm{sat}_{\underline{w},\bar{w}}(\boldsymbol{w}_{k-1})]$ is bounded. Therefore, there exits a positive number m_w, which satisfies

$$\frac{\varpi_{1,k}}{\varpi_{2,k}^3} g_1 s_{\phi,k} \tilde{\boldsymbol{w}}_k^T \boldsymbol{\xi}_k + \frac{g_1}{2\gamma_2} g_1 \tilde{\boldsymbol{w}}_k^T \tilde{\boldsymbol{w}}_k \leq m_w. \tag{35}$$

Similarly, it follows from (26), (27) and (28) that there exists positive numbers m_ϑ, m_ρ and m_ϱ meeting

$$\begin{aligned} & \frac{\varpi_{1,k}}{\varpi_{2,k}^3} s_{\phi,k} g_1 \tilde{\boldsymbol{\vartheta}}_k^T \boldsymbol{\varphi}_k + \frac{g_1}{2\gamma_3}\tilde{\boldsymbol{\vartheta}}_k^T \tilde{\boldsymbol{\vartheta}}_k \\ & = \frac{g_1}{2\gamma_3}[-\boldsymbol{\vartheta}_k^T \boldsymbol{\vartheta}_k + \boldsymbol{\vartheta}^{*T} \boldsymbol{\vartheta}^* - 2\boldsymbol{\vartheta}^T \mathrm{sat}_{\underline{\vartheta},\bar{\vartheta}}(\boldsymbol{\vartheta}_{k-1}) \\ & \quad + 2\boldsymbol{\vartheta}_k^T \mathrm{sat}_{\underline{\vartheta},\bar{\vartheta}}(\boldsymbol{\vartheta}_{k-1})] \\ & = -\frac{g_1}{2\gamma_3}[\boldsymbol{\vartheta}_k - \mathrm{sat}_{\underline{\vartheta},\bar{\vartheta}}(\boldsymbol{\vartheta}_{k-1})]^T [\boldsymbol{\vartheta}_k - \mathrm{sat}_{\underline{\vartheta},\bar{\vartheta}}(\boldsymbol{\vartheta}_{k-1})] \\ & \quad + \frac{g_1}{2\gamma_3}[\mathrm{sat}_{\underline{\vartheta},\bar{\vartheta}}(\boldsymbol{\vartheta}_{k-1}^T)\mathrm{sat}_{\underline{\vartheta},\bar{\vartheta}}(\boldsymbol{\vartheta}_{k-1}) + \boldsymbol{\vartheta}^{*T} \boldsymbol{\vartheta}^* \\ & \quad - 2\boldsymbol{\vartheta}^T \mathrm{sat}_{\underline{\vartheta},\bar{\vartheta}}(\boldsymbol{\vartheta}_{k-1})] \\ & \leq \frac{g_1}{2\gamma_3}[\mathrm{sat}_{\underline{\vartheta},\bar{\vartheta}}(\boldsymbol{\vartheta}_{k-1}^T)\mathrm{sat}_{\underline{\vartheta},\bar{\vartheta}}(\boldsymbol{\vartheta}_{k-1}) + \boldsymbol{\vartheta}^{*T} \boldsymbol{\vartheta}^* \\ & \quad - 2\boldsymbol{\vartheta}^T \mathrm{sat}_{\underline{\vartheta},\bar{\vartheta}}(\boldsymbol{\vartheta}_{k-1})] \\ & \leq m_\vartheta, \end{aligned} \tag{36}$$

$$\begin{aligned} & \frac{\varpi_{1,k}}{|\varpi_{2,k}|^3}|s_{\phi,k}| g_1 \tilde{\rho}_k x_{1,k}^2 |u_{1,k}| + \frac{g_1}{2\gamma_4}\tilde{\rho}_k^2 \\ & = \frac{g_1}{2\gamma_4}[-\rho_k^2 + \rho^2 - 2\rho \mathrm{sat}_{\underline{\rho},\bar{\rho}}(\rho_{k-1}) + 2\rho_k \mathrm{sat}_{\underline{\rho},\bar{\rho}}(\rho_{k-1})] \end{aligned}$$

$$
\begin{aligned}
&= \frac{g_1}{2\gamma_4}[\mathrm{sat}_{\underline{\rho},\bar{\rho}}(\rho_{k-1})\mathrm{sat}_{\underline{\rho},\bar{\rho}}(\rho_{k-1}) + \rho^2 - 2\rho\mathrm{sat}_{\underline{\rho},\bar{\rho}}(\rho_{k-1})] \\
&\quad -\frac{g_1}{2\gamma_4}[\rho_k - \mathrm{sat}_{\underline{\rho},\bar{\rho}}(\rho_{k-1})]^2 \\
&\le \frac{g_1}{2\gamma_4}[\mathrm{sat}_{\underline{\rho},\bar{\rho}}(\rho_{k-1})\mathrm{sat}_{\underline{\rho},\bar{\rho}}(\rho_{k-1}) + \rho^2 - 2\rho\mathrm{sat}_{\underline{\rho},\bar{\rho}}(\rho_{k-1})] \\
&\le m_\rho
\end{aligned} \tag{37}
$$

and

$$
\begin{aligned}
&\frac{\varpi_{1,k}}{|\varpi_{2,k}|^3}|s_{\phi,k}|\tilde{\varrho}_k + \frac{1}{2\gamma_5}\tilde{\varrho}_k^2 \\
&= \frac{1}{2\gamma_5}[-\varrho_k^2 + \varrho^2 - 2\varrho\mathrm{sat}_{\underline{\varrho},\bar{\varrho}}(\varrho_{k-1}) + 2\varrho_k\mathrm{sat}_{\underline{\varrho},\bar{\varrho}}(\varrho_{k-1})] \\
&= \frac{1}{2\gamma_5}[\mathrm{sat}_{\underline{\varrho},\bar{\varrho}}(\varrho_{k-1})\mathrm{sat}_{\underline{\varrho},\bar{\varrho}}(\varrho_{k-1}) + \varrho^2 - 2\varrho\mathrm{sat}_{\underline{\varrho},\bar{\varrho}}(\varrho_{k-1})] \\
&\quad -\frac{1}{2\gamma_5}[\varrho_k - \mathrm{sat}_{\underline{\varrho},\bar{\varrho}}(\varrho_{k-1})]^2 \\
&\le \frac{1}{2\gamma_5}[\mathrm{sat}_{\underline{\varrho},\bar{\varrho}}(\varrho_{k-1})\mathrm{sat}_{\underline{\varrho},\bar{\varrho}}(\varrho_{k-1}) + \varrho^2 - 2\varrho\mathrm{sat}_{\underline{\varrho},\bar{\varrho}}(\varrho_{k-1})] \\
&\le m_\varrho,
\end{aligned} \tag{38}
$$

respectively. Substituting (34)-(38) into (33) yields

$$
\dot{L}_k \le -\frac{\varpi_{1,k}^2}{\varpi_{2,k}^2}\gamma_{1,k}g_1 s_{\phi,k}^2 + m_w + m_\vartheta + m_\rho + m_\varrho. \tag{39}
$$

Note that $s_{\phi,k}(0) = 0$ and then $L_k(0) = 0$. From (39), we have

$$
\begin{aligned}
L_k(t) &\le L_k(0) - \int_0^t \frac{\varpi_{1,k}^2}{\varpi_{2,k}^2}\gamma_{1,k}g_1 s_{\phi,k}^2 d\tau + t(m_w + m_\vartheta \\
&\quad + m_\rho + m_\varrho) \\
&\le t(m_w + m_\vartheta + m_\rho + m_\varrho)
\end{aligned} \tag{40}
$$

From (40), we have

$$
\frac{1}{2}\frac{s_{\phi k}^2(t)}{(b_s^2 - s_{\phi,k}^2(t))^2} \le t(m_w + m_\vartheta + m_\rho + m_\varrho). \tag{41}
$$

Due to $s_{\phi,k}(0) = 0$ for $k = 0, 1, 2, 3, \cdots$, from (41), we can see $|s_{\phi k}(t)| < b_s$ holds for $t \in [0, T]$. Suppose $|s_{\phi,k}(t)| \to b_{s-}$ holds at a certain moment $t_\delta \in (0, T]$. Then,

$$
\frac{1}{2}\frac{s_{\phi k}^2(t_\delta)}{(b_s^2 - s_{\phi,k}^2(t_\delta))^2} \to +\infty, \tag{42}
$$

would happen, which is contrary to (41). Actually, from (41), we can deduce

$$
b_s^2 - s_{\phi,k}^2(t) \ge \frac{|s_{\phi k}(t)|}{\sqrt{2t(m_w + m_\vartheta + m_\rho + m_\varrho)}}. \tag{43}
$$

According to (43), we thus get

$$
\begin{aligned}
|s_{\phi,k}(t)| &\le \sqrt{b_s^2 - \frac{|s_{\phi k}(t)|}{\sqrt{2t(m_w + m_\vartheta + m_\rho + m_\varrho)}}} \\
&< b_s.
\end{aligned} \tag{44}
$$

Further, according to the definition of s_k, we have

$$
|s_k(t)| \le |s_k(0)|\mathrm{e}^{-\mu t} + |s_{\phi,k}(t)| < |s_k(0)|\mathrm{e}^{-\mu t} + b_s. \tag{45}
$$

From (40), we can see that $L_k(t)$ is bounded, which further leads to the boundedness of s_k, $\boldsymbol{e}_k$, $\boldsymbol{x}_k$, $\boldsymbol{\xi}_k$ and $\boldsymbol{\varphi}_k$. By the property of saturation functions, $\boldsymbol{w}_k$, $\boldsymbol{\vartheta}_k$, ρ_k and ϱ_k are also guaranteed to be bounded. On basis of above conclusions, we can deduce that $u_{1,k}$ is bounded from (23). Then, $u_{2,k}$, u_k and all other signals can be verified to be bounded.

Part B. The convergence of tracking error

On the basis of (31) and (32), we have

$$
\begin{aligned}
L_k \le &-\int_0^t \gamma_1 g_1 \frac{\varpi_{1,k}}{\varpi_{2,k}^2}s_{\phi,k}^2 d\tau + \int_0^t \frac{\varpi_{1,k}}{\varpi_{2,k}^3}s_{\phi,k} \\
&\times g_1(\tilde{\boldsymbol{w}}_k^T\boldsymbol{\xi}_k + \tilde{\boldsymbol{\vartheta}}_k^T\boldsymbol{\varphi}_k)d\tau + \int_0^t \frac{\varpi_{1,k}}{|\varpi_{2,k}|^3}\big(|s_{\phi,k}|g_1 \\
&\times\tilde{\rho}_k x_{1,k}^2|u_{1,k}| + |s_{\phi,k}|g_1\tilde{\varrho}_k\big)d\tau \\
&+\frac{g_1}{2\gamma_2}\int_0^t \tilde{\boldsymbol{w}}_k^T\tilde{\boldsymbol{w}}_k d\tau + \frac{g_1}{2\gamma_3}\int_0^t \tilde{\boldsymbol{\vartheta}}_k^T\tilde{\boldsymbol{\vartheta}}_k d\tau \\
&+\frac{g_1}{2\gamma_4}\int_0^t \tilde{\rho}_k^2 d\tau + \frac{g_1}{2\gamma_5}\int_0^t \tilde{\varrho}_k^2 d\tau.
\end{aligned} \tag{46}
$$

While $k > 0$, from (46), we can derive

$$
\begin{aligned}
&L_k - L_{k-1} \\
&\le -\int_0^t \gamma_1 g_1 \frac{\varpi_{1,k}}{\varpi_{2,k}^2}s_{\phi,k}^2 d\tau + \int_0^t \frac{s_{\phi,k}(\varpi_{1,k})}{\varpi_{2,k}^3} \\
&\quad\times g_1(\tilde{\boldsymbol{w}}_k^T\boldsymbol{\xi}_k + \tilde{\boldsymbol{\vartheta}}_k^T\boldsymbol{\varphi}_k)d\tau + \int_0^t \frac{\varpi_{1,k}}{|\varpi_{2,k}|^3}\big(|s_{\phi,k}|g_1 \\
&\quad\times\tilde{\rho}_k x_{1,k}^2|u_{1,k}| + |s_{\phi,k}|g_1\tilde{\varrho}_k\big)d\tau \\
&\quad+\frac{g_1}{2\gamma_2}\int_0^t (\tilde{\boldsymbol{w}}_k^T\tilde{\boldsymbol{w}}_k - \tilde{\boldsymbol{w}}_{k-1}^T\tilde{\boldsymbol{w}}_{k-1})d\tau + \frac{g_1}{2\gamma_3}\int_0^t (\tilde{\boldsymbol{\vartheta}}_k^T\tilde{\boldsymbol{\vartheta}}_k \\
&\quad-\tilde{\boldsymbol{\vartheta}}_{k-1}^T\tilde{\boldsymbol{\vartheta}}_{k-1})d\tau + \frac{g_1}{2\gamma_4}\int_0^t (\tilde{\rho}_k^2 - \tilde{\rho}_{k-1}^2)d\tau \\
&\quad+\frac{g_1}{2\gamma_5}\int_0^t (\tilde{\varrho}_k^2 - \tilde{\varrho}_{k-1}^2)d\tau + V_k(0) - V_{k-1}.
\end{aligned} \tag{47}
$$

Note that in (47), $V_k(0) = 0$. By using the relationship $(\upsilon - q)^2 - (\upsilon - \varsigma)^2 \le (\upsilon - q)^2 - (\upsilon - \mathrm{sat}_{\underline{\varsigma},\bar{\varsigma}}(\varsigma))^2$, from (25), we obtain

$$
\begin{aligned}
&\frac{g_1}{2\gamma_2}(\tilde{\boldsymbol{w}}_k^T\tilde{\boldsymbol{w}}_k - \tilde{\boldsymbol{w}}_{k-1}^T\tilde{\boldsymbol{w}}_{k-1}) + g_1\frac{s_{\phi,k}(\varpi_{1,k})}{\varpi_{2,k}^3}\tilde{\boldsymbol{w}}_k^T\boldsymbol{\xi}_k \\
&\le \frac{g_1}{2\gamma_2}[(\boldsymbol{w} - \boldsymbol{w}_k)^T(\boldsymbol{w} - \boldsymbol{w}_k) - (\boldsymbol{w} - \mathrm{sat}_{\underline{w},\bar{w}}(\boldsymbol{w}_{k-1}))^T(\boldsymbol{w} \\
&\quad-\mathrm{sat}_{\underline{w},\bar{w}}(\boldsymbol{w}_{k-1}))] + g_1\frac{s_{\phi,k}(\varpi_{1,k})}{\varpi_{2,k}^3}\tilde{\boldsymbol{w}}_k^T\boldsymbol{\xi}_k \\
&\le \frac{g_1}{2\gamma_2}(2\boldsymbol{w} - \boldsymbol{w}_k - \mathrm{sat}_{\underline{w},\bar{w}}(\boldsymbol{w}_{k-1}))^T(\mathrm{sat}_{\underline{w},\bar{w}}(\boldsymbol{w}_{k-1}) - \boldsymbol{w}_k) \\
&\quad+g_1\frac{s_{\phi,k}(\varpi_{1,k})}{\varpi_{2,k}^3}\tilde{\boldsymbol{w}}_k^T\boldsymbol{\xi}_k \\
&\le \frac{g_1}{\gamma_2}(\boldsymbol{w} - \boldsymbol{w}_k)^T[\mathrm{sat}_{\underline{w},\bar{w}}(\boldsymbol{w}_{k-1}) - \boldsymbol{w}_k + \frac{\gamma_2 s_{\phi,k}(\varpi_{1,k})\boldsymbol{\xi}_k}{\varpi_{2,k}^3}] \\
&= 0.
\end{aligned} \tag{48}
$$

From (26), we have

$$\begin{aligned}
&\frac{g_1}{2\gamma_2}(\tilde{\boldsymbol{\vartheta}}_k^T\tilde{\boldsymbol{\vartheta}}_k-\tilde{\boldsymbol{\vartheta}}_{k-1}^T\tilde{\boldsymbol{\vartheta}}_{k-1})+g_1\frac{s_{\phi,k}(\varpi_{1,k})}{\varpi_{2,k}^3}\tilde{\boldsymbol{\vartheta}}_k^T\boldsymbol{\varphi}_k\\
&\le\frac{g_1}{2\gamma_2}[(\boldsymbol{\vartheta}^*-\boldsymbol{\vartheta}_k)^T(\boldsymbol{\vartheta}^*-\boldsymbol{\vartheta}_k)-(\boldsymbol{\vartheta}^*-\mathrm{sat}_{\underline{\vartheta},\bar{\vartheta}}(\boldsymbol{\vartheta}_{k-1}))^T(\boldsymbol{\vartheta}^*\\
&\quad-\mathrm{sat}_{\underline{\vartheta},\bar{\vartheta}}(\boldsymbol{\vartheta}_{k-1}))]+g_1\frac{s_{\phi,k}(\varpi_{1,k})}{\varpi_{2,k}^3}\tilde{\boldsymbol{\vartheta}}_k^T\boldsymbol{\varphi}_k\\
&\le\frac{g_1}{2\gamma_2}(2\boldsymbol{\vartheta}^*-\boldsymbol{\vartheta}_k-\mathrm{sat}_{\underline{\vartheta},\bar{\vartheta}}(\boldsymbol{\vartheta}_{k-1}))^T(\mathrm{sat}_{\underline{\vartheta},\bar{\vartheta}}(\boldsymbol{\vartheta}_{k-1})-\boldsymbol{\vartheta}_k)\\
&\quad+g_1\frac{s_{\phi,k}(\varpi_{1,k})}{\varpi_{2,k}^3}\tilde{\boldsymbol{\vartheta}}_k^T\boldsymbol{\varphi}_k\\
&\le\frac{g_1}{\gamma_2}(\boldsymbol{\vartheta}^*-\boldsymbol{\vartheta}_k)^T\Big[\mathrm{sat}_{\underline{\vartheta},\bar{\vartheta}}(\boldsymbol{\vartheta}_{k-1})-\boldsymbol{\vartheta}_k+\gamma_2\frac{s_{\phi,k}(\varpi_{1,k})}{\varpi_{2,k}^3}\boldsymbol{\varphi}_k\Big]\\
&=0. \qquad (49)
\end{aligned}$$

Similarly, from (27) and (28), we can obtain

$$\begin{aligned}
&\frac{g_1}{2\gamma_4}(\tilde{\rho}_k^2-\tilde{\rho}_{k-1}^2)+\frac{g_1\tilde{\rho}_k|s_{\phi,k}|x_{1,k}^2|u_{1,k}|(\varpi_{1,k})}{|\varpi_{2,k}|^3}\\
&\le\frac{g_1}{\gamma_4}(\rho-\rho_k)\Big[\mathrm{sat}_{0,\bar{\rho}}(\rho_{k-1})-\rho_k+\gamma_4|s_{\phi,k}|x_{1,k}^2|u_{1,k}|\\
&\quad\times\frac{\varpi_{1,k}}{|\varpi_{2,k}|^3}\Big]\\
&=0 \qquad (50)
\end{aligned}$$

and

$$\begin{aligned}
&\frac{g_1}{2\gamma_5}(\tilde{\varrho}_k^2-\tilde{\varrho}_{k-1}^2)+\frac{g_1|s_{\phi,k}|\tilde{\varrho}_k(\varpi_{1,k})}{|\varpi_{2,k}|^3}\\
&\le\frac{g_1}{\gamma_5}(\varrho-\varrho_k)\Big[\mathrm{sat}_{0,\bar{\varrho}}(\varrho_{k-1})-\varrho_k+\frac{\gamma_5|s_{\phi,k}|(\varpi_{1,k})}{|\varpi_{2,k}|^3}\Big]\\
&=0, \qquad (51)
\end{aligned}$$

respectively. Substituting (48)-(51) into (47) yields

$$L_k(t)-L_{k-1}(t)\le-V_{k-1}(t) \qquad (52)$$

By using the recursive relation (52) and the definition of V_{k-1}, we can further obtain

$$L_k(t)\le L_0(t)-\frac{1}{2}\sum_{j=0}^{k-1}s_{\phi,j}^2(t) \qquad (53)$$

for $k>0$.

It can be seen from (40) that $L_0(t)$ is bounded for $t\in[0,T]$. Therefore, there exists a positive constant m_L, which satisfies the equality as follows:

$$L_0\le m_L. \qquad (54)$$

Combining (53) with (54), we can draw a conclusion that

$$\lim_{k\to+\infty}s_{\phi,k}(t)=0 \qquad (55)$$

holds for all $t\in[0,T]$, which means

$$\lim_{k\to+\infty}|s_k(t)|\le|s_k(0)|\mathrm{e}^{-\mu t},\forall t\in[0,T]. \qquad (56)$$

TABLE 1. Parameters in the PAM system.

Parameters			
$k_0=0.9$	$k_1=1$	$k_2=1.5$	$k_3=4$
$k_u=1$	$\epsilon_0=0.5$	$b_v=2$	$r=4cm$
$l_0=20cm$	$u_p=2.5V$	$J=10kg\cdot cm^2$	

By using the relationship

$$\dot{e}_{1,k}+\lambda e_{1,k}=s_k, \qquad (57)$$

from (56), we can obtain

$$|e_{1,k}(t)|=\mathrm{e}^{-\lambda t}|e_{1,k}(0)|+\frac{\mathrm{e}^{-\mu t}-\mathrm{e}^{-\lambda t}}{\lambda-\mu}|s_k(0)| \qquad (58)$$

as the iteration number k increases. Therefore, by choosing proper positive numbers λ and μ, $|e_{1,k}(t)|$ may exponentially converge with respect to t. ■

In this work, difference learning method is applied to estimate unknown parameters, the optimal weight of FLS, and the upper bound of the sum of approximation error and noncontinuous disturbance. Since the uncertain input gain contains angle state signal and unknown parameters, it is difficult to design iterative learning controller through direct estimating all contained unknown parameters. Robust control strategy is used to deal with this difficulty during controller design.

V. NUMERICAL SIMULATION

To verify the correctness of above theoretical analysis, numerical simulation was performed for the PAM system (6), where $d_v(\theta,\dot{\theta},t)=2+0.5x_1^2x_2^2+0.8\sin(x_{1,j})x_{2,j}+0.2\mathrm{sgn}(x_{1,j}x_{2,j})+0.2\mathrm{rand}_1$, $[x_{1,k}(0),x_{2,k}(0)=[0.7+0.1\mathrm{rand}_2,-0.05+0,05\mathrm{rand}_3]^T$ and the model parameters are listed in TABLE 1. The control objective is to let $x_{1,k}$ track the reference trajectory $x_{1,d}=0.5\cos(\frac{\pi}{2.5}t)$ under the condition that $x_{1,k}(0)\neq x_{1,d}(0)$ and $x_{2,k}(0)\neq x_{2,d}(0)$. Here, rand_1, rand_2 and rand_3 denote random numbers between 0 and 1.

In the implementation, seven fuzzy sets are characterized by the following membership functions.

$$\begin{aligned}
\mu_{\mathcal{F}_i^1}(x_{i,k})&=\exp[-\frac{1}{2}(\frac{x_{i,k}+1.5}{0.7})^2],\\
\mu_{\mathcal{F}_i^2}(x_{i,k})&=\exp[-\frac{1}{2}(\frac{x_{i,k}+1}{0.7})^2],\\
\mu_{\mathcal{F}_i^3}(x_{i,k})&=\exp[-\frac{1}{2}(\frac{x_{i,k}+0.5}{0.7})^2],\\
\mu_{\mathcal{F}_i^4}(x_{i,k})&=\exp[-\frac{1}{2}(\frac{x_{i,k}}{0.7})^2],\\
\mu_{\mathcal{F}_i^5}(x_{i,k})&=\exp[-\frac{1}{2}(\frac{x_{i,k}-0.5}{0.7})^2],\\
\mu_{\mathcal{F}_i^6}(x_{i,k})&=\exp[-\frac{1}{2}(\frac{x_{i,k}-1}{0.7})^2],\\
\mu_{\mathcal{F}_i^7}(x_{i,k})&=\exp[-\frac{1}{2}(\frac{x_{i,k}-1.5}{0.7})^2],\quad i=1,2.
\end{aligned}$$

The control parameters and gains in control law (22) and learning laws (25)-(26) are set as follows: $\lambda=2,\mu=5$,

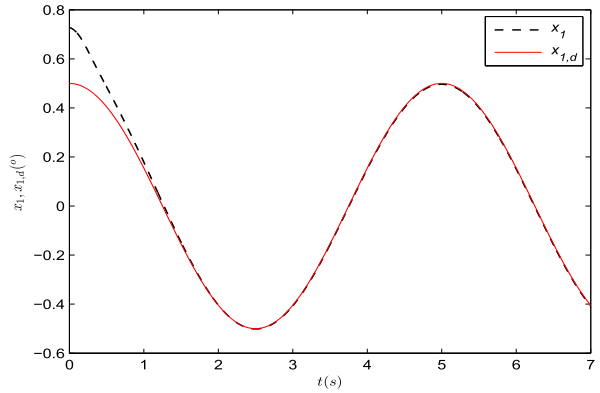

FIGURE 2. x_1 and its reference signal $x_{1,d}$(constraint ILC).

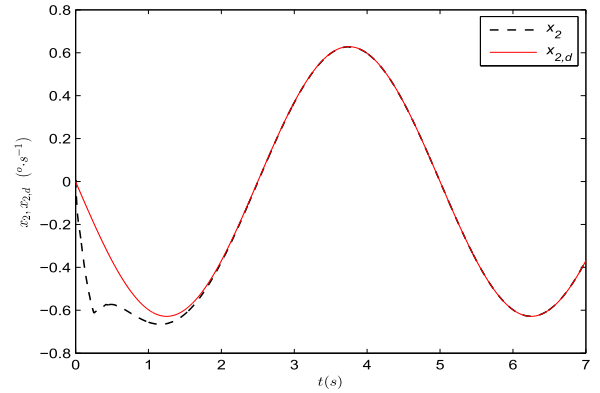

FIGURE 3. x_2 and its reference signal $x_{2,d}$ (constraint ILC).

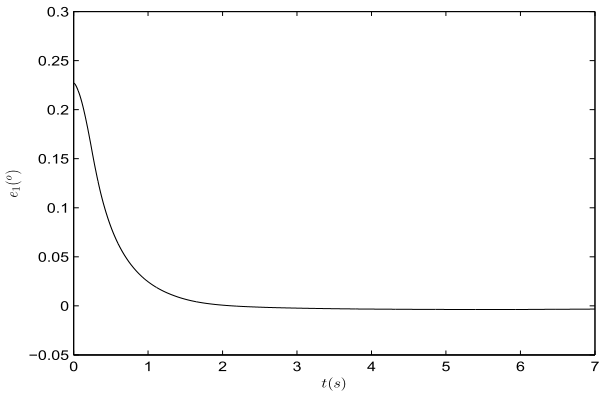

FIGURE 4. The error e_1 (constraint ILC).

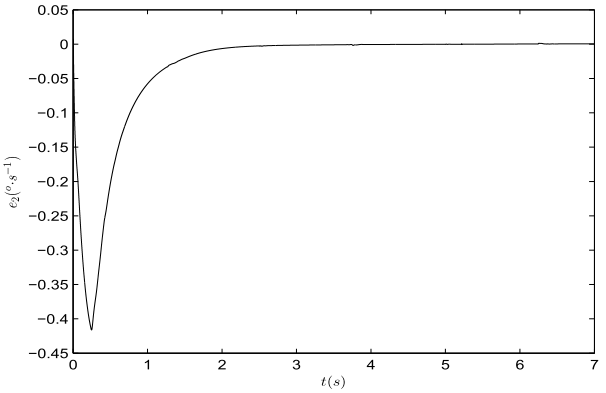

FIGURE 5. The error e_2 (constraint ILC).

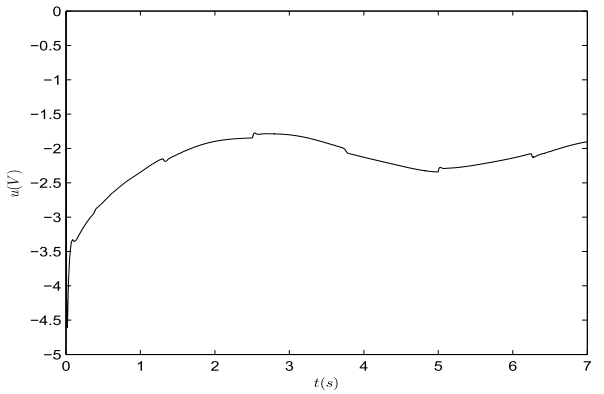

FIGURE 6. Control input(constraint ILC).

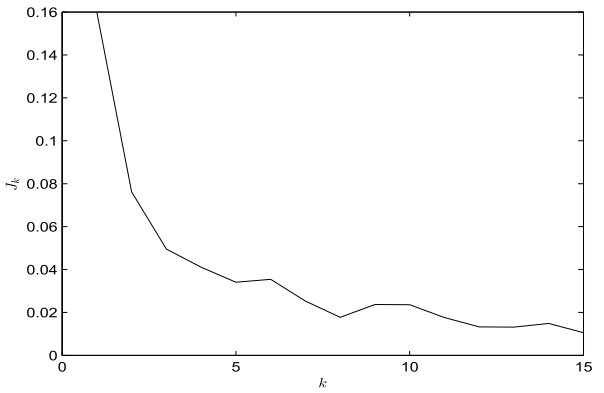

FIGURE 7. History of $s_{\phi,k}$ convergence(constraint ILC).

$\gamma_1 = 5, \gamma_2 = 1, \gamma_3 = 1, \mu_4 = 0.01, \mu_5 = 0.01, b_s = 0.25, T = 7s$. After 15 iteration cycles, the simulation results are shown in Figs. 2-7. Figs. 2-3 show the profiles of angle position and angular velocity at the 15th learning cycle, respectively. The corresponding tracking error profiles presented in Figs. 4-5, respectively. From Figs. 2-5, we conclude that $\boldsymbol{x} = [x_{1,k}, x_{2,k}]^T$ can precisely track $\boldsymbol{x}_d(t) = [x_{1,d}, x_{2,d}]^T$. The control input at the 15th learning cycle is shown in Fig. 6. Fig. 7 gives the convergence history of $s_{\phi,k}$ in the filtering-error constrained ILC, where $J_k \triangleq \max_{t\in[0,T]} |s_{\phi,k}|$. From Fig. 7, we can see that the constraint $s_{\phi,k} < b_s$ holds for each iteraion.

To verify the effectiveness of our proposed ILC algorithm, two comparison examples are provided in the following part.

Comparison A: To verify the constraint property of our proposed ILC algorithm, the simulation applying non-constraint adaptive ILC (60)-(65) is studied for PAM system (6).

$$u_k = u_{1,k} + u_{2,k}, \tag{59}$$

$$u_{1,k} = -\gamma_1 s_{\phi,k} - \boldsymbol{w}_k^T \boldsymbol{\xi}_k - \boldsymbol{\vartheta}_k^T \boldsymbol{\varphi}_k, \tag{60}$$

$$u_{2,k} = -(\rho_k x_1^2 |u_{1,k}| + \varrho_k) \mathrm{sat}_{-1,1}\left(\frac{s_k(t)}{\phi_k(t)}\right) \tag{61}$$

$$\boldsymbol{w_k} = \mathrm{sat}_{\underline{w},\bar{w}}(\boldsymbol{w}_{k-1}) + \gamma_2 s_{\phi,k} \boldsymbol{\xi}_k, \boldsymbol{w_{-1}} = 0, \tag{62}$$

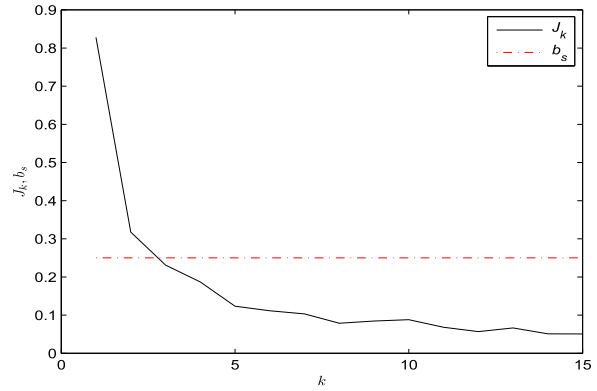

FIGURE 8. History of $s_{\phi,k}$ convergence(unconstraint ILC).

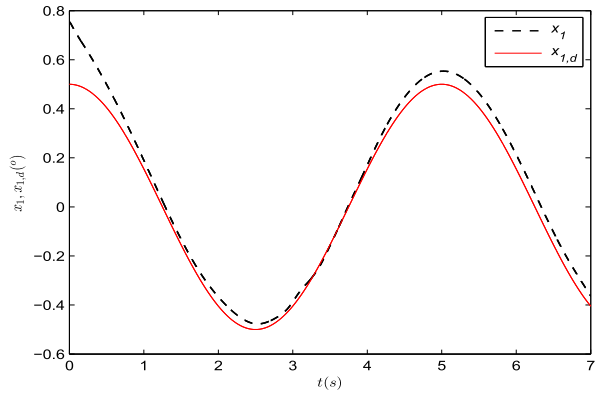

FIGURE 9. x_1 and its reference signal $x_{1,d}$(time-invariant boundary layer based ILC).

$$\boldsymbol{\vartheta_k} = \text{sat}_{\underline{\vartheta},\bar{\vartheta}}(\boldsymbol{\vartheta}_{k-1}) + \gamma_3 s_{\phi,k}\boldsymbol{\varphi}_k, \boldsymbol{\vartheta_{-1}} = 0, \quad (63)$$

$$\rho_k = \text{sat}_{0,\bar{\rho}}(\rho_{k-1}) + \gamma_4 |s_{\phi,k}| x_{1,k}^2 |u_{1,k}|, \rho_{-1} = 0, \quad (64)$$

$$\varrho_k = \text{sat}_{0,\bar{\varrho}}(\varrho_{k-1}) + \gamma_5 |s_{\phi,k}|, \varrho_{-1} = 0. \quad (65)$$

The control parameters here are set as $\lambda = 2, \mu = 5, \gamma_1 = 5, \gamma_2 = 1, \gamma_3 = 1, \mu_4 = 0.01, \mu_5 = 0.01$ and $T = 7s$. Fig. 8 shows that $|s_{\phi,k}|$ converges to a tunable residual set as the iteration increases, but the constraint inequality $s_{\phi,k} < b_s$ is violated. The definition of J_k in Fig. 8 is the same as the one in Fig. 7. Comparing Fig. 7 with Fig. 8, we can see that our constraint adaptive ILC algorithm is effective in both error convergence and system error constraint.

Comparison B: To show the necessity of dealing with initial position problem, the robust adaptive ILC algorithm based on time-invariant boundary layer is adopted for simulation.

$$u_k = u_{1,k} + u_{2,k}, \quad (66)$$

$$u_{1,k} = -\gamma_1 s_{\eta,k} - \boldsymbol{w}_k^T \boldsymbol{\xi}_k - \boldsymbol{\vartheta}_k^T \boldsymbol{\varphi}_k, \quad (67)$$

$$u_{2,k} = -(\rho_k x_1^2 |u_{1,k}| + \varrho_k)\text{sat}_{-1,1}\left(\frac{s_k}{\eta}\right) \quad (68)$$

$$\boldsymbol{w_k} = \text{sat}_{\underline{w},\bar{w}}(\boldsymbol{w}_{k-1}) + \gamma_2 s_{\eta,k}\boldsymbol{\xi}_k, \boldsymbol{w_{-1}} = 0, \quad (69)$$

$$\boldsymbol{\vartheta_k} = \text{sat}_{\underline{\vartheta},\bar{\vartheta}}(\boldsymbol{\vartheta}_{k-1}) + \gamma_3 s_{\eta,k}\boldsymbol{\varphi}_k, \boldsymbol{\vartheta_{-1}} = 0, \quad (70)$$

$$\rho_k = \text{sat}_{0,\bar{\rho}}(\rho_{k-1}) + \gamma_4 |s_{\eta,k}| x_{1,k}^2 |u_{1,k}|, \rho_{-1} = 0, \quad (71)$$

$$\varrho_k = \text{sat}_{0,\bar{\varrho}}(\varrho_{k-1}) + \gamma_5 |s_{\eta,k}|, \varrho_{-1} = 0, \quad (72)$$

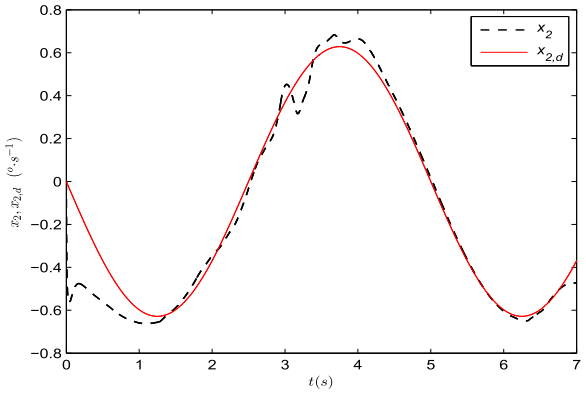

FIGURE 10. x_2 and its reference signal $x_{2,d}$(time-invariant boundary layer based ILC).

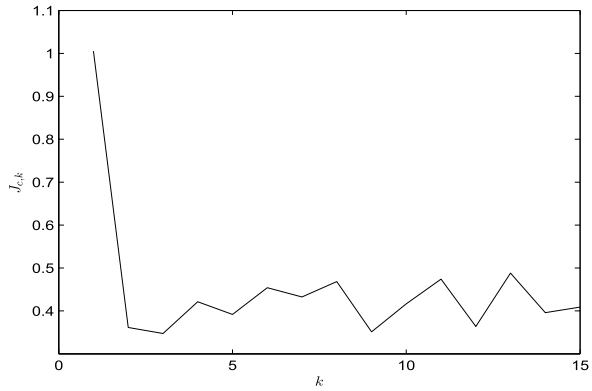

FIGURE 11. Maximum of $|s_{\eta,k}|$ in the iteration domain(time-invariant boundary layer based ILC).

where $s_{\eta,k} = s_k - \eta \text{sat}_{-1,1}(\frac{s_k}{\eta})$, η is a positive constant. Set $\eta = 0.1$, and other control parameters are set as same as the one in *Comparison A*. Figs. 9-10 show the profiles of angle position and angular velocity at the 15th learning cycle, respectively. Fig. 11 shows that the maximum of $|s_{\eta,k}|$ in the iteration domain, where $J_{c,k} \triangleq \max_{t\in[0,T]} |s_{\eta,k}|$. cannot be obtained as the iteration increases. From Figs.9-11, we can see that the tracking control performance is not satisfied. These simulation results verify the effectiveness of our proposed filtering-error constrained adaptive ILC scheme.

VI. CONCLUSION

A filtering-error constrained adaptive learning fuzzy control scheme is proposed to solve the tracking problem of PAM systems in this paper. To achieve system constraint in iterations, a new type of barrier Lyapunov function is introduced in controller design. The initial position problem of ILC for PAM systems is handled by using the technique of time-varying boundary layer. The continuous nonparametric uncertainties in the PAM system is compensated by the adaptive leaning FLS, whose optimal weight is estimated by difference learning approach. It is shown that the angle tracking error and angular velocity tracking error can asymptotically converge to a tunable residual set as the iteration number goes to infinity.

REFERENCES

[1] D. Liang, N. Sun, Y. Wu, Y. Chen, Y. Fang, and L. Liu, "Energy-based motion control for pneumatic artificial muscle actuated robots with experiments," *IEEE Trans. Ind. Electron.*, vol. 69, no. 7, pp. 7295–7306, Jul. 2022, doi: 10.1109/TIE.2021.3095788.

[2] H. Yang, Y. Yu, and J. Zhang, "Angle tracking of a pneumatic muscle actuator mechanism under varying load conditions," *Control Eng. Pract.*, vol. 61, pp. 1–10, Apr. 2017.

[3] L. Zhao, H. Cheng, J. Zhang, and Y. Xia, "Angle attitude control for a 2-DOF parallel mechanism of PMAs using tracking differentiators," *IEEE Trans. Ind. Electron.*, vol. 66, no. 11, pp. 8659–8669, Nov. 2019.

[4] G. Andrikopoulos, G. Nikolakopoulos, and S. Manesis, "Advanced nonlinear PID-based antagonistic control for pneumatic muscle actuators," *IEEE Trans. Ind. Electron.*, vol. 61, no. 12, pp. 6926–6937, Dec. 2014.

[5] K. Xing, Q. Xu, J. Huang, Y. Wang, J. He, and J. Wu, "Tracking control of pneumatic artificial muscle actuators based on sliding mode and nonlinear disturbance observer," *IET Control Theory Appl.*, vol. 4, no. 10, pp. 2058–2070, Oct. 2010.

[6] N. Sun, D. Liang, Y. Wu, Y. Chen, Y. Qin, and Y. Fang, "Adaptive control for pneumatic artificial muscle systems with parametric uncertainties and unidirectional input constraints," *IEEE Trans. Ind. Informat.*, vol. 16, no. 2, pp. 969–979, Feb. 2020.

[7] J.-P. Cai, F. Qian, R. Yu, and L. Shen, "Adaptive control for a pneumatic muscle joint system with saturation input," *IEEE Access*, vol. 8, pp. 117698–117705, 2020.

[8] J. Huang, J. Qian, L. Liu, Y. Wang, C. Xiong, and S. Ri, "Echo state network based predictive control with particle swarm optimization for pneumatic muscle actuator," *J. Franklin Inst.*, vol. 353, no. 12, pp. 2761–2782, Aug. 2016.

[9] L. Zhao, H. Cheng, Y. Xia, and B. Liu, "Angle tracking adaptive backstepping control for a mechanism of pneumatic muscle actuators via an AESO," *IEEE Trans. Ind. Electron.*, vol. 66, no. 6, pp. 4566–4576, Jun. 2019.

[10] D. Zhang, X. Zhao, and J. Han, "Active model-based control for pneumatic artificial muscle," *IEEE Trans. Ind. Electron.*, vol. 64, no. 2, pp. 1686–1695, Feb. 2017.

[11] R. Chi, X. Liu, R. Zhang, Z. Hou, and B. Huang, "Constrained data-driven optimal iterative learning control," *J. Process Control*, vol. 55, pp. 10–29, Jul. 2017.

[12] D. Huang, W. Yang, T. Huang, N. Qin, Y. Chen, and Y. Tan, "Iterative learning operation control of high-speed trains with adhesion dynamics," *IEEE Trans. Control Syst. Technol.*, vol. 29, no. 6, pp. 2598–2608, Nov. 2021, doi: 10.1109/TCST.2021.3049958.

[13] B. Jia, S. Liu, and Y. Liu, "Visual trajectory tracking of industrial manipulator with iterative learning control," *Ind. Robot, Int. J.*, vol. 42, no. 1, pp. 54–63, Jan. 2015.

[14] D. Meng and J. Zhang, "Robust optimization-based iterative learning control for nonlinear systems with nonrepetitive uncertainties," *IEEE/CAA J. Autom. Sinica*, vol. 8, no. 5, pp. 1001–1014, May 2021.

[15] D. Shen, "Iterative learning control with incomplete information: A survey," *IEEE/CAA J. Autom. Sinica*, vol. 5, no. 5, pp. 885–901, Jul. 2018.

[16] J. Liu, X. Ruan, and Y. Zheng, "Iterative learning control for discrete-time systems with full learnability," *IEEE Trans. Neural Netw. Learn. Syst.*, vol. 33, no. 2, pp. 629–643, Feb. 2022.

[17] Y. Wang, E. Dassau, and F. J. Doyle, "Closed-loop control of artificial pancreatic β-cell in type 1 diabetes mellitus using model predictive iterative learning control," *IEEE Trans. Biomed. Eng.*, vol. 57, no. 2, pp. 211–219, Feb. 2010.

[18] T. Hu, K. H. Low, L. Shen, and X. Xu, "Effective phase tracking for bioinspired undulations of robotic fish models: A learning control approach," *IEEE/ASME Trans. Mechatronics*, vol. 19, no. 1, pp. 191–200, Feb. 2014.

[19] X. Li, J.-X. Xu, and D. Huang, "An iterative learning control approach for linear systems with randomly varying trial lengths," *IEEE Trans. Autom. Control*, vol. 59, no. 7, pp. 1954–1960, Jul. 2014.

[20] X. Bu, Q. Yu, Z. Hou, and W. Qian, "Model free adaptive iterative learning consensus tracking control for a class of nonlinear multiagent systems," *IEEE Trans. Syst., Man, Cybern., Syst.*, vol. 49, no. 4, pp. 677–686, Apr. 2019.

[21] J. Li and J. Li, "Distributed adaptive fuzzy iterative learning control of coordination problems for higher order multi-agent systems," *Int. J. Syst. Sci.*, vol. 47, no. 10, pp. 2318–2329, Feb. 2015.

[22] G. Li, Y. Han, T. Lu, D. Chen, and H. Chen, "Iterative learning control for nonlinear multi-agent systems with initial shifts," *IEEE Access*, vol. 8, pp. 144343–144351, 2020.

[23] X. Dai and X. Zhou, "Mixed PD-type iterative learning control algorithm for a class of parabolic singular distributed parameter systems," *IEEE Access*, vol. 9, pp. 12180–12190, 2021.

[24] W. Cao, J. Qiao, and M. Sun, "Consensus control via iterative learning for singular multi-agent systems with switching topologies," *IEEE Access*, vol. 9, pp. 81412–81420, 2021.

[25] C.-J. Chien, C.-T. Hsu, and C.-Y. Yao, "Fuzzy system-based adaptive iterative learning control for nonlinear plants with initial state errors," *IEEE Trans. Fuzzy Syst.*, vol. 12, no. 5, pp. 724–732, Oct. 2004.

[26] X.-D. Li, M.-M. Lv, and J. K. L. Ho, "Adaptive ILC algorithms of nonlinear continuous systems with non-parametric uncertainties for non-repetitive trajectory tracking," *Int. J. Syst. Sci.*, vol. 47, no. 10, pp. 2279–2289, 2016.

[27] Q. Z. Yan, M. X. Sun, and H. Li, "Iterative learning control for nonlinear uncertain systems with arbitrary initial state," *Acta Autom. Sinica*, vol. 42, no. 4, pp. 545–555, Apr. 2016.

[28] J.-X. Xu, X. Jin, and D. Huang, "Composite energy function-based iterative learning control for systems with nonparametric uncertainties," *Int. J. Adapt. Control Signal Process.*, vol. 28, no. 1, pp. 1–13, 2014.

[29] X. Jin and J.-X. Xu, "A barrier composite energy function approach for robot manipulators under alignment condition with position constraints," *Int. J. Robust Nonlinear Control*, vol. 24, no. 17, pp. 2840–2851, 2014.

[30] G. Zhu, X. Wu, Q. Yan, and J. Cai, "Robust learning control for tank gun control servo systems under alignment condition," *IEEE Access*, vol. 7, pp. 145524–145531, 2019.

[31] Q. Ai, D. Ke, J. Zuo, W. Meng, Q. Liu, Z. Zhang, and S. Q. Xie, "High-order model-free adaptive iterative learning control of pneumatic artificial muscle with enhanced convergence," *IEEE Trans. Ind. Electron.*, vol. 67, no. 11, pp. 9548–9559, Nov. 2020.

[32] D. Guo, W. Wang, Y. Zhang, Q. Yan, and J. Cai, "Angle tracking robust learning control for pneumatic artificial muscle systems," *IEEE Access*, vol. 9, pp. 142232–142238, 2021.

[33] E. G. Gilbert and K. T. Tan, "Linear systems with state and control constraints: The theory and application of maximal output admissible sets," *IEEE Trans. Autom. Control*, vol. 36, no. 9, pp. 1008–1020, Sep. 1991.

[34] D. Q. Mayne, J. B. Rawlings, C. V. Rao, and P. O. M. Scokaert, "Constrained model predictive control: Stability and optimality," *Automatica*, vol. 36, no. 6, pp. 789–814, 2000.

[35] K. Kogiso and K. Hirata, "Reference governor for constrained systems with time-varying references," in *Proc. IEEE Int. Conf. Multisensor Fusion Integr. Intell. Syst.*, Sep. 2006, pp. 359–364.

[36] X. Jin, Z. Wang, and R. H. S. Kwong, "Convex optimization based iterative learning control for iteration-varying systems under output constraints," in *Proc. 11th IEEE Int. Conf. Control Autom. (ICCA)*, Jun. 2014, pp. 1444–1448.

[37] K. B. Ngo, R. Mahony, and Z.-P. Jiang, "Integrator backstepping using barrier functions for systems with multiple state constraints," in *Proc. 44th IEEE Conf. Decis. Control*, 2005, pp. 8306–8312.

[38] L. Liu, Y. J. Liu, S. C. Tong, and C. L. P. Chen, "Integral barrier Lyapunov function-based adaptive control for switched nonlinear systems," *Sci. China Inf. Sci.*, vol. 63, no. 3, pp. 1–14, 2020.

[39] X. Jin and J.-X. Xu, "Iterative learning control for output-constrained systems with both parametric and nonparametric uncertainties," *Automatica*, vol. 49, no. 8, pp. 2508–2516, 2013.

[40] Q. Z. Yan and M. X. Sun, "Error-tracking iterative learning control with state constrained for nonparametric uncertain systems," *Control Theory Appl.*, vol. 32, no. 7, pp. 895–901, Jul. 2015.

[41] Q. Yu, Z. Hou, and R. Chi, "Adaptive iterative learning control for nonlinear uncertain systems with both state and input constraints," *J. Franklin Inst.*, vol. 353, no. 15, pp. 3920–3943, Oct. 2016.

[42] X. Jin, "Iterative learning control for non-repetitive trajectory tracking of robot manipulators with joint position constraints and actuator faults," *Int. J. Adapt. Control Signal Process.*, vol. 31, no. 6, pp. 859–875, Jun. 2017.

[43] L. X. Wang, *A Course in Fuzzy Systems*. Upper Saddle River, NJ, USA: Prentice-Hall, 1999.

[44] J. Cai, C. Wen, L. Xing, and Q. Yan, "Decentralized backstepping control for interconnected systems with non-triangular structural uncertainties," *IEEE Trans. Autom. Control*, early access, Feb. 16, 2022, doi: 10.1109/TAC.2022.3152083.

[45] W. Qi, G. Zong, and W. X. Zheng, "Adaptive event-triggered SMC for stochastic switching systems with semi-Markov process and application to boost converter circuit model," *IEEE Trans. Circuits Syst. I, Reg. Papers*, vol. 68, no. 2, pp. 786–796, Feb. 2021.

[46] W. Qi, J. H. Park, G. Zong, J. Cao, and J. Cheng, "Filter for positive stochastic nonlinear switching systems with phase-type semi-Markov parameters and application," *IEEE Trans. Syst., Man, Cybern., Syst.*, vol. 52, no. 4, pp. 2225–2236, Apr. 2022.
[47] H. He, W. Qi, Z. Liu, and M. Wang, "Adaptive attack-resilient control for Markov jump system with additive attacks," *Nonlinear Dyn.*, vol. 103, no. 2, pp. 1585–1598, Jan. 2021.
[48] X. Zheng and X. Yang, "Command filter and universal approximator based backstepping control design for strict-feedback nonlinear systems with uncertainty," *IEEE Trans. Autom. Control*, vol. 65, no. 3, pp. 1310–1317, Mar. 2020.
[49] J. Kong, B. Niu, Z. Wang, P. Zhao, and W. Qi, "Adaptive output-feedback neural tracking control for uncertain switched MIMO nonlinear systems with time delays," *Int. J. Syst. Sci.*, vol. 52, no. 13, pp. 2813–2830, Oct. 2021.

XIAOHUI GUAN received the master's degree in computer science from Zhejiang University, Hangzhou, China, in 2005. She is currently an Associate Professor with the College of Information Engineering, Zhejiang University of Water Resources and Electric Power. Her current research interests include machine learning and adaptive control.

ZHONGJIE HE (Member, IEEE) received the B.S. degree in automation from Hangzhou Dianzi University, Hangzhou, China, in 2003, and the Ph.D. degree in electrical engineering from Zhejiang University, Hangzhou, in 2009. From 2009 to 2012, he worked as an Electrical Engineer at the Zhejiang Electric Power Planning and Design Institute, State Grid, Hangzhou. Since 2012, he has been working as a Lecturer at the College of Automation, Hangzhou Dianzi University. His current research interests include artificial intelligence, adaptive control, scheduling optimization, and muti-objective programming. He is a member of the Chinese Association of Artificial Intelligence and the Director of the IEEE PES Electric Vehicle Satellite Committee-China.

MEIYAN ZHANG was born in Sanmen, Taizhou, Zhejiang, China, in 1983. She received the B.S. and master's degrees from the Zhejiang University of Technology, Hangzhou, China, in 2006 and 2009, respectively. She then joined a postgraduate program at the Institute of Automation, Zhejiang University of Technology. From 2016 to 2017, she was a Visiting Research Scholar at Missouri University, Rolla, MO, USA. She joined the College of Electrical Engineering, Zhejiang University of Water Resources and Electric Power, as an Associate Professor. In recent years, she has published more than 20 papers on wireless sensor networks and holds more than ten patents. Her research interests include wireless communication, wireless sensor networks, and multimedia sensor networks.

HUIJIE XIA is currently pursuing the B.S. degree in the IoT engineering with the College of Information Engineering, Zhejiang University of Water Resources and Electric Power, Hangzhou, China. His current research interests include embedded system development and nonlinear system control.